Hindawi
Discrete Dynamics in Nature and Society
Volume 2019, Article ID 8743482, 11 pages
https://doi.org/10.1155/2019/8743482

Research Article

Projective Synchronization of Nonidentical Fractional-Order Memristive Neural Networks

Chong Chen and Zhixia Ding

School of Electrical and Information Engineering, Wuhan Institute of Technology, Wuhan 430205, China

Correspondence should be addressed to Zhixia Ding; zxding89@163.com

Received 15 May 2019; Revised 4 July 2019; Accepted 15 July 2019; Published 1 August 2019

Academic Editor: Ewa Pawluszewicz

This paper investigates projective synchronization of nonidentical fractional-order memristive neural networks (NFMNN) via sliding mode controller. Firstly, based on the sliding mode control theory, a new fractional-order integral sliding mode controller is designed to ensure the occurrence of sliding motion. Furthermore, according to fractional-order differential inequalities and fractional-order Lyapunov direct method, the trajectories of the system converge to the sliding mode surface to carry out sliding mode motion, and some sufficient criteria are obtained to achieve global projective synchronization of NFMNN. In addition, the conclusions extend and improve some previous works on the synchronization of fractional-order memristive neural networks (FMNN). Finally, a simulation example is given to verify the effectiveness and correctness of the obtained results.

1. Introduction

In 1971, Professor Chua theoretically predicted the existence of memristive element [1]. In the following years, his team presented the basic characteristics, synthesis principles, and applications of memristor [2, 3]. Until 2008, researchers from Hewlett-Packard Co. firstly made nanomemristor devices, which triggered an upsurge in memristor research [4]. As the fourth basic circuit element, memristor has the characteristics that the other three basic components (resistance, capacitance, and inductance) cannot replicate. It can not only remember the number of charges flowing through it, but change its resistance by controlling the change of current. What is more important, these capabilities can be maintained even when power is cut off. Therefore, memristor has broadened application prospects in computer science [5], bioengineering [6], neural networks [7], electronic engineering [8], communication engineering [9], and so on.

Neural networks have the abilities of self-learning and self-adapting through training. The design of weights is crucial for neural networks. The hardware implementation of weight requires a long-term memory. With the development of memristor, it is feasible to introduce memristor into neural networks to solve the above problem. At present, the memristive neural networks (MNN) have been widely studied in information processing [10], image processing [11], artificial intelligence [12], and other fields [13–15]. As we all know, fractional-order calculus is a generalization of traditional integer-order calculus. Fractional-order calculus is not local and can describe memory property of neuron and dependence of the historical data. Meanwhile, fractional-order models can describe and model a real system more accurately than the classical integer-order models [16, 17]. By introducing fractional-order differential operators into integer-order MNN model, a new fractional-order memristive neural networks (FMNN) model can be established. Such systems can truly reflect the essential features of the system and extend the capability of neural networks. So far, many researchers have devoted themselves to investigating FMNN and a series of results about FMNN have appeared, such as [18–23].

It was Huygens, the inventor of pendulum, who discovered synchronization for the first time. Until 1990, Pecora and Carroll of the U.S. Naval Laboratory put forward the master-slave chaotic synchronization scheme, which realized the synchronization of two chaotic systems in the circuit and promoted the theoretical study of chaotic synchronization and chaotic control [24]. So far, there are many types of synchronization, such as complete synchronization [25–27], antisynchronization [28], lag synchronization [29, 30],

generalized synchronization [31], projective synchronization [32–35], and phase and antiphase synchronization [36]. The scale factor of projective synchronization can be set flexibly, which enhances the uncertainty of slave system and improves communication security. Therefore, it is necessary to investigate projective synchronization of FMNN.

To the best of our knowledge, the existing results of projective synchronization about FMNN are identical system. In fact, functions and parameters of master-slave system are often mismatched, which is inevitable. Although various forms of control strategies have been designed to solve the problems of system's synchronization [25, 27, 30, 37–40], they are difficult to deal with projective synchronization of NFMNN. In order to solve such problems, the fractional-order sliding mode controller is introduced, which can overcome the uncertainty of systems and has strong robustness to disturbance, especially for the control of nonlinear systems. The sliding mode controller needs the following three elements: firstly, any trajectories reach the sliding mode surface in free time; secondly, there is a sliding mode region on the sliding mode surface; thirdly, the sliding mode motion is asymptotic stable.

Motivated by the above discussions, we focus on the projective synchronization of nonidentical fractional-order memristive neural networks in this paper. The main contributions of this paper are as follows: (1) In this paper, projective synchronization of NFMNN is studied by designing a new type of fractional-order integral sliding mode controller. (2) By using the fractional-order differential inequality and fractional-order Lyapunov direct method, the projective synchronization criteria of NFMNN are obtained. At the same time, the obtained criteria can realize the complete synchronization and antisynchronization of NFMNN, stability, and projective synchronization of FMNN. (3) Comparing with the conclusions in [25, 33], our results on projective synchronization of FMNN achieve a valuable improvement and are less conservative.

The structure of this paper is summarized as follows. Some preliminaries and the system models are given in Section 2. In Section 3, some sufficient criteria are obtained to achieve global projective synchronization of NFMNN. In Section 4, the validity and correctness of the obtained results are illustrated by numerical simulation. Finally, conclusions are drawn in Section 5.

2. Preliminaries and System Description

2.1. Caputo Fractional-Order Calculus

Definition 1 (see [41]). The fractional-order integral of order α for an integrable function $f(t) : [0, +\infty] \longrightarrow \mathbb{R}$ is defined as

$$ {}_0I_t^{\alpha} f(t) = \frac{1}{\Gamma(\alpha)} \int_0^t (t-\xi)^{\alpha-1} f(\xi)\, d\xi, \quad t \geq 0, \tag{1} $$

where $t \geq 0$, $\alpha > 0$, and $\Gamma(\cdot)$ is the Gamma function which is defined as

$$ \Gamma(x) = \int_0^{\infty} e^{-t} t^{x-1} dt, \quad \mathrm{Re}(x) > 0. \tag{2} $$

Definition 2 (see [41]). The Caputo fractional-order derivative of order α for a function $f(t) \in C^{n+1}([0, +\infty], \mathbb{R})$ is defined by

$$ {}_0^C D_t^{\alpha} f(t) = \frac{1}{\Gamma(n-\alpha)} \int_0^t \frac{f^{(n)}(\xi)}{(t-\xi)^{\alpha-n+1}} d\xi, \tag{3} $$

where $t \geq 0$ and $n-1 < \alpha < n \in \mathbb{N}_+$. Particularly, when $0 < \alpha < 1$,

$$ {}_0^C D_t^{\alpha} f(t) = \frac{1}{\Gamma(1-\alpha)} \int_0^t \frac{f'(\xi)}{(t-\xi)^{\alpha}} d\xi. \tag{4} $$

A series of significant properties about fractional-order calculus are listed as follows [41].

Property 3. For any constants v_1 and v_2, the linearity of Caputo fraction-order calculus is expressed by

$$ \begin{aligned} &{}_0^C D_t^{\alpha} \left(v_1 \cdot f(t) + v_2 \cdot g(t) \right) \\ &\quad = v_1 \cdot {}_0^C D_t^{\alpha} f(t) + v_2 \cdot {}_0^C D_t^{\alpha} g(t). \end{aligned} \tag{5} $$

Property 4. If $w(t) \in C^1[0, T]$, $T > 0$, then

$$ {}_0^C D_t^{\alpha}\, {}_0^C D_t^{\beta} w(t) = {}_0^C D_t^{\beta}\, {}_0^C D_t^{\alpha} w(t) = {}_0^C D_t^{\alpha+\beta} w(t), \quad t \in [0, T]. \tag{6} $$

where $\alpha > 0$, $\beta > 0$, and $\alpha + \beta \leq 1$.

Lemma 5 (see [32]). *If $w(t) \in C^1([0, +\infty), \mathbb{R})$, then the following inequality holds almost everywhere:*

$$ {}_0^C D_t^{\alpha} |w(t)| \leq \mathrm{sgn}(w(t))\, {}_0^C D_t^{\alpha} w(t), \quad 0 < \alpha < 1. \tag{7} $$

Lemma 6 (see [42]). *Let $x(t) \in \mathbb{R}$ be a continuous and derivable function. Then, for any $t \geq 0$, one have*

$$ \frac{1}{2}\, {}_0^C D_t^{\alpha} x^2(t) \leq x(t)\, {}_0^C D_t^{\alpha} x(t), \quad \alpha \in (0, 1). \tag{8} $$

By applying Lemma 6, the following formula can be obtained:

$$ \frac{1}{2}\, {}_0^C D_t^{\alpha} x^T(t)\, x(t) \leq x^T(t)\, {}_0^C D_t^{\alpha} x(t), \tag{9} $$

where $x(t) \in \mathbb{R}^n$, $\alpha \in (0, 1)$, and $t \geq 0$.

2.2. System Description.

In this section, we consider a class of FMNN as the master system, which is described by the following equation:

$$ {}_0^C D_t^{\alpha} x_i(t) = -c_i x_i(t) + \sum_{i=1}^{n} a_{ij} \left(x_j(t) \right) f_j \left(x_j(t) \right) + I_i, \tag{10} $$

where $\alpha \in (0, 1)$, $x(t) = (x_1(t), x_2(t), \ldots, x_n(t))^T \in \mathbb{R}^n$, $x_i(t)$ denotes the state variable associated with the ith neuron, $i \in \mathbb{N}_+$, $t \geq 0$; $c_i > 0$ is self-regulation parameters of neurons; I_i is a constant of the external input; $f_i(t)$ denotes nonlinear

activation function; $a_{ij}(x_j(t))$ express connection memristive weights, defined by

$$a_{ij}\left(x_j(t)\right) = \begin{cases} a_{ij}^{*} & \left|x_j(t)\right| > T_j \\ co\left\{a_{ij}^{*}, a_{ij}^{\circ}\right\} & \left|x_j(t)\right| = T_j \\ a_{ij}^{\circ} & \left|x_j(t)\right| < T_j, \end{cases} \tag{11}$$

where $i \in \mathbb{N}_+$, $T_j > 0$ denotes switching of memristor, and a_{ij}^{*} and a_{ij}° are any constants. And the matrix form of the master system is given by

$${}_0^C D_t^{\alpha} x(t) = -Cx(t) + Af(x(t)) + I, \tag{12}$$

where $C = \mathrm{diag}(c_1, c_2, \ldots, c_n)$, $A = (a_{ij}(x_j(t)))_{n\times n}$, and $I = (I_1, I_2, \ldots, I_n)^T$.

Similarly, the corresponding slave system is described as

$${}_0^C D_t^{\alpha} y(t) = -Dy(t) + Bg\left(y(t)\right) + H + u(t), \tag{13}$$

where $u(t)$ is the control input; $D = \mathrm{diag}(d_1, d_2, \ldots, d_n)$, $d_i > 0$; $H = (H_1, H_2, \ldots, H_n)^T$ is the external input vector; $B = (b_{ij}(y_j(t)))_{n\times n}$, $b_{ij}(y_j(t))$ are expressed as

$$b_{ij}\left(y_j(t)\right) = \begin{cases} b_{ij}^{*} & \left|y_j(t)\right| > T_j \\ co\left\{b_{ij}^{*}, b_{ij}^{\circ}\right\} & \left|y_j(t)\right| = T_j \\ b_{ij}^{\circ} & \left|y_j(t)\right| < T_j. \end{cases} \tag{14}$$

Assuming that the measurement output of system (12) depends on the instantaneous state, the form is as follows:

$$z(t) = Mx(t), \tag{15}$$

where $z(t) \in \mathbb{R}^m$ and $M \in \mathbb{R}^{m\times n}$ is known constant matrix.

Compared with continuous fractional-order neural networks, the FMNN is discontinued on the right-hand side because of the introduction of memristor. To deal with this problem, we consider the concept of Filippov solution in this paper.

Definition 7 (see [43]). In the Filippov sense, a function $x(t) = (x_1(t), x_2(t), \ldots, x_n(t))^T$ is a solution of system (12) on $[0, +\infty)$ with initial condition $x(0) = (x_1(0), x_2(0), \ldots, x_n(0))^T$, if $x(t)$ is absolutely continuous on any compact interval of $[0, +\infty)$, $x(0) = (x_1(0), x_2(0), \ldots, x_n(0))^T$ and

$${}_0^C D_t^{\alpha} x_i(t) \in -c_i x_i(t) + \sum_{j=1}^{n} co\left[a_{ij}\left(x_j(t)\right)\right] f_j\left(x_j(t)\right) + I_i, \tag{16}$$

for $t \geq 0$, $i \in \mathbb{N}_+$, where $0 < \alpha < 1$, or there exist $\theta_{ij}[x_j(t)] \in co[a_{ij}(x_j(t))]$ such that

$${}_0^C D_t^{\alpha} x_i(t) = -c_i x_i(t) + \sum_{j=1}^{n} \theta_{ij}\left[x_j(t)\right] f_j\left(x_j(t)\right) + I_i, \tag{17}$$

where

$$co\left[a_{ij}\left(x_j(t)\right)\right] = \begin{cases} a_{ij}^{*} & \left|x_j(t)\right| > T_j \\ co\left\{a_{ij}^{*}, a_{ij}^{\circ}\right\} & \left|x_j(t)\right| = T_j \\ a_{ij}^{\circ} & \left|x_j(t)\right| < T_j \end{cases}, \quad t \in [0, +\infty),\ i \in \mathbb{N}_+. \tag{18}$$

And in the same way, we can obtain

$${}_0^C D_t^{\alpha} y_i(t) \in -d_i y_i(t) + \sum_{j=1}^{n} co\left[b_{ij}\left(y_j(t)\right)\right] g_j\left(y_j(t)\right) + H_i + u_i(t), \tag{19}$$

where $t \geq 0$, $i \in \mathbb{N}_+$, and $0 < \alpha < 1$, or there exist $\omega_{ij}[y_j(t)] \in co[b_{ij}(y_j(t))]$ such that

$${}_0^C D_t^{\alpha} y_i(t) = -d_i y_i(t) + \sum_{j=1}^{n} \omega_{ij}\left[y_j(t)\right] g_j\left(y_j(t)\right) + H_i + u_i(t), \tag{20}$$

where

$$co\left[b_{ij}\left(y_j(t)\right)\right] = \begin{cases} b_{ij}^{*} & \left|y_j(t)\right| > T_j \\ co\left\{b_{ij}^{*}, b_{ij}^{\circ}\right\} & \left|y_j(t)\right| = T_j \\ b_{ij}^{\circ} & \left|y_j(t)\right| < T_j, \end{cases} \quad t \in [0, +\infty),\ i \in \mathbb{N}_+. \tag{21}$$

In order to guarantee the existence and uniqueness of the solution of system (12) and (13) or fractional-order differential inclusions (17) and (20), the following assumptions are provided.

Assumption 8. For a.a. $j \in \mathbb{N}_+$, there exist Lipschitz constants $F_j > 0, G_j > 0$; for any $v_1 \neq v_2 \in \mathbb{R}$, the following conditions are always established:

$$\left|f_j(v_1) - f_j(v_2)\right| \leq F_j\left|v_1 - v_2\right|, \tag{22}$$

and

$$\left|g_j(v_1) - g_j(v_2)\right| \leq G_j\left|v_1 - v_2\right|. \tag{23}$$

Assumption 9. $f_j(x)$ and $g_j(x)$ are bounded on $\mathbb{R}$. Meanwhile, $f_j(\pm T_j) = g_j(\pm T_j) = 0$.

Definition 10 (see [32]). If there exists a nonzero constant ξ for any solution $x(t)$ and $y(t)$ of master system (12) and slave system (13), respectively, one obtains

$$\lim_{t\longrightarrow+\infty} \left\|y(t) - \xi x(t)\right\| = 0, \tag{24}$$

then the globally asymptotically projective synchronization of the master system (12) and slave system (13) can be realized, where $\|\cdot\|$ denotes the Euclidean norm and ξ denotes the projective coefficient.

Remark 11. If $\xi = -1$, the global antisynchronization of system (12) and (13) can be attainable. If $\xi = 1$, system (12) and (13) can achieve globally asymptotically complete synchronization. If $\xi = 0$, there is the following form: $\lim_{t\to+\infty} \| y(t) \| = 0$, which shows that the slave system (13) is globally asymptotically stabilized to the origin.

2.3. Mittag-Leffler Stability. In this part, the Mittag-Leffler function and Mittag-Leffler stability are given by the following content.

Definition 12 (see [41]). The Mittag-Leffler function with two parameters is defined as

$$E_{\alpha,\beta}(x) = \sum_{l=0}^{\infty} \frac{x^l}{\Gamma(l\alpha+\beta)}, \quad \alpha > 0,\ \beta > 0,\ x \in \mathbb{C}. \tag{25}$$

For $\beta = 0$, we have $E_\alpha(x) = E_{\alpha,1}(x)$ defined as

$$E_\alpha(x) = \sum_{l=0}^{\infty} \frac{x^l}{\Gamma(l\alpha+1)} \quad \alpha > 0,\ x \in \mathbb{C}. \tag{26}$$

Definition 13 (see [25]). If $x(t) = x^*$ is an equilibrium point of the system (12), and there are two constants $\Xi > 0$ and $\Upsilon > 0$ for any solution $x(t)$ of FMNN (12) with initial value $x(0)$, one has

$$x \left\| (t) - x^* \right\| \le \Xi \left\| x(0) - x^* \right\| E_\alpha\left(-\Upsilon t^\alpha\right), \quad t \ge 0. \tag{27}$$

In particular, $x^* = 0$, and one has

$$\|x(t)\| \le \Xi \|x(0)\| E_\alpha\left(-\Upsilon t^\alpha\right), \quad t \ge 0. \tag{28}$$

Definition 14 (see [25]). System (12) is expected to be globally Mittag-Leffler stable, if its equilibrium point is Mittag-Leffler stable.

Lemma 15 (see [32]). *For x^* is an equilibrium point of the FMNN (12), if there is a Lyapunov function $V(t, x(t)) : [0, +\infty) \times \mathbb{D} \in \mathbb{R}^n$ and class-κ function $\vartheta_i (i = 1, 2, 3)$ satisfying*

$$\begin{aligned} &\vartheta_1(\|x(t)\|) \le V(t, x(t)) \le \vartheta_2(\|x(t)\|), \\ &{}_0^C D_t^\alpha V(t, x(t)) \le -\vartheta_3(\|x(t)\|), \end{aligned} \tag{29}$$

where $\alpha \in (0, 1)$ and the origin is included in a domain of $\mathbb{D} \subseteq \mathbb{R}^n$, so the equilibrium point of the FMNN (12) is asymptotically stable.

3. Main Results

The synchronization error is defined as $e(t) = y(t) - \xi x(t)$. From the master system (12) and slave system (13), the error system is described by

$$\begin{aligned} {}_0^C D_t^\alpha e(t) = {} & -De(t) + B^* g(e(t) + \xi x(t)) \\ & - \widehat{B}^* g(\xi x(t)) + \xi (C - D) x(t) \\ & + \widehat{B}^* g(\xi x(t)) - \xi A^* f(x(t)) + H - \xi I \\ & + u(t), \end{aligned} \tag{30}$$

where $B^* = (\omega_{ij}[y_j(t)])_{n\times n}$, $\widehat{B}^* = (\omega_{ij}[\xi x_j(t)])_{n\times n}$, and $A^* = (\theta_{ij}[x_j(t)])_{n\times n}$. Based on Definition 10, the problem of projective synchronization for NFMNN is transformed into the problem of asymptotic stability of error systems (30).

In this part, a fractional-order integral sliding mode controller is designed to deal with the problem of projective synchronization of NFMNN. The sliding mode surface is defined as

$$\begin{aligned} S(t) = {} & e(t) + {}_0 I_t^\alpha \left\{ Ce(t) \right. \\ & - \left[B^* g(e(t) + \xi x(t)) - \widehat{B}^* g(\xi x(t)) \right] \\ & \left. + N\left(My(t) - \xi z(t)\right) \right\} = e(t) \\ & + {}_0 I_t^\alpha \left\{ - \left[B^* g(e(t) + \xi x(t)) - \widehat{B}^* g(\xi x(t)) \right] \right. \\ & \left. + (C + NM) e(t) \right\}, \end{aligned} \tag{31}$$

where $S(t) = (S_1(t), S_2(t), \ldots, S_n(t))^T$; C, B^*, and $\widehat{B}^*$ are defined in the master system (12) and the slave system (20), respectively; $N \in \mathbb{R}^{n\times m}$ is denoted as the gain matrix which can be selected appropriately; $M \in \mathbb{R}^{m\times n}$ is the coefficient matrix in (15).

According to the theory of sliding mode control [44], for the sake of the error system (30) operating on the sliding mode, the sliding surface and its derivative must satisfy $S(t) = 0$ and $\dot{S}(t) = 0$.

Based on Property 4, one has

$$\dot{S}(t) = {}_0^C D_t^{1-\alpha} {}_0^C D_t^\alpha S(t) = 0, \tag{32}$$

which implies that

$${}_0^C D_t^\alpha S(t) = 0, \tag{33}$$

Assume that Assumptions 8 and 9 hold; expression (31) can be written as

$$\begin{aligned} {}_0^C D_t^\alpha S(t) = {} & {}_0^C D_t^\alpha e(t) - \left[B^* g(y(t)) - \widehat{B}^* g(\xi x(t)) \right] \\ & + (C + NM) e(t). \end{aligned} \tag{34}$$

Substituting (30) into (34) and combining (33), then

$$\begin{aligned} {}_0^C D_t^\alpha S(t) = {} & (-D + C + NM) e(t) + \xi (C - D) x(t) \\ & + \widehat{B}^* g(\xi x(t)) - \xi A^* f(x(t)) + H - \xi I \\ & + u(t) = 0. \end{aligned} \tag{35}$$

By means of (35), an equivalent control law can be written as

$$\begin{aligned} u_q(t) = {} & -(-D + C + NM) e(t) - \xi (C - D) x(t) \\ & - H - \widehat{B}^* g(\xi x(t)) + \xi A^* f(x(t)) + \xi I. \end{aligned} \tag{36}$$

Combining (30) with (36), the dynamics of sliding mode can be written as

$$\begin{aligned} {}_0^C D_t^\alpha e(t) = {} & -(C + NM) e(t) \\ & + \left[B^* g(e(t) + \xi x(t)) - \widehat{B}^* g(\xi x(t)) \right], \end{aligned} \tag{37}$$

and obviously, $e^* = 0$ is an equilibrium point of the sliding mode dynamics (37).

On account of the sliding mode control theory, a reaching law is denoted as

$$u_p = -\delta\left(\operatorname{sgn}\left(S\left(t\right)\right)\right), \tag{38}$$

where

$$\operatorname{sgn}\left(S_i\left(t\right)\right) = \begin{cases} 1, & S_i\left(t\right) > 0 \\ 0, & S_i\left(t\right) = 0 \\ -1, & S_i\left(t\right) < 0, \end{cases} \quad i = 1, 2, \ldots, n \in N^+, \tag{39}$$

and $\delta > 0$ is the switching gain. Lastly, the sliding mode controller $u(t)$ is designed as

$$\begin{aligned} u\left(t\right) &= u_q\left(t\right) + u_p\left(t\right) \\ &= -\left(-D + C + NM\right)e\left(t\right) - \xi\left(C - D\right)x\left(t\right) \\ &\quad + \xi A^* f\left(x\left(t\right)\right) - \widehat{B}^* g\left(\xi x\left(t\right)\right) - H + \xi I \\ &\quad - \sigma \operatorname{sgn}\left(S\left(t\right)\right). \end{aligned} \tag{40}$$

Remark 16. As mentioned in [45, 46], some undesirable dynamic properties may be produced owing to the discontinuous function $\operatorname{sgn}(S(t))$ existing in the sliding mode control system (40). To deal with the problem of the harmful chattering, the $\operatorname{sgn}(S(t))$ is replaced by a continuous function $\tanh(S(t))$. Hence, the sliding mode control (40) is altered as follows:

$$\begin{aligned} u\left(t\right) &= u_q\left(t\right) + u_p\left(t\right) \\ &= -\left(-D + C + NM\right)e\left(t\right) - \xi\left(C - D\right)x\left(t\right) \\ &\quad + \xi A^* f\left(x\left(t\right)\right) - \widehat{B}^* g\left(\xi x\left(t\right)\right) - H + \xi I \\ &\quad - \sigma \tanh\left(S\left(t\right)\right). \end{aligned} \tag{41}$$

Theorem 17. *Assume that the sliding model surface is denoted by (31) and Assumption 9 holds; the trajectories of error system (30) can be asymptotically driven on the switching surface $S(t) = 0$ based on the sliding model controller (40).*

Proof. Constructing the positive definite function as a Lyapunov function candidate

$$V = \frac{1}{2}S^T\left(t\right)S\left(t\right), \tag{42}$$

in view of Lemma 6 and Definition 2, expression (42) can be written as

$$\begin{aligned} {}_0^C D_t^{\alpha} V\left(t\right) &= {}_0^C D_t^{\alpha}\frac{1}{2}S^T\left(t\right)S\left(t\right) \le S^T\left(t\right){}_0^C D_t^{\alpha} S\left(t\right) \\ &= \sum_{i=1}^{n} S_i\left(t\right)\cdot\left(-\sigma\right)\cdot\operatorname{sgn}\left(S_i\left(t\right)\right) \\ &= -\sigma\left\|S\left(t\right)\right\|_1, \end{aligned} \tag{43}$$

where $\|\cdot\|_1$ denotes the 1-norm.

Based on Lemma 15, when $\sigma > 0$ holds, the trajectories of system can asymptotically converge to $S(t) = 0$, which means that the trajectories of the error system are driven to the designed sliding mode surface and stayed on it at any subsequent moment. This obtains the proof. □

In order to analyze the stability of the sliding motion, the following assumption is given as follows.

Assumption 18. For a.a. $i \in \mathbb{N}_+$, one has

$$-c_i + \sum_{j=1}^{n}\left(\sum_{k=1}^{m}\left|N_{jk}M_{ki}\right|\right) + \sum_{j=1}^{n}\left|b_{ji}^{\heartsuit}\right|G_i < 0, \tag{44}$$

where $c_i > 0$ is the constant in the master system (17); N_{jk} denotes the gain of system (31); M_{ki} is the coefficient of the system (15); $|b_{ji}^{\heartsuit}| = \max\{|b_{ji}^*|, |b_{ji}^\circ|\}$; and G_i is the Lipschitz constants of function $g(\cdot)$ in the Assumption 8.

Theorem 19. *In the case of Assumptions 8, 9, and 18, system (37) is globally asymptotically stable.*

Proof. Firstly, expression (37) can be written as

$$\begin{aligned} {}_0^C D_t^{\alpha} e_i\left(t\right) &= -c_i e_i\left(t\right) - \sum_{j=1}^{n}\sum_{k=1}^{m} N_{ik}M_{kj}e_j\left(t\right) \\ &\quad + \sum_{j=1}^{n}\left\{\omega_{ij}\left[y_j\left(t\right)\right]g_j\left(y_j\left(t\right)\right)\right. \\ &\quad \left. - \omega_{ij}\left[\xi x_j\left(t\right)\right]g_j\left(\xi x_j\left(t\right)\right)\right\}. \end{aligned} \tag{45}$$

Constructing the function $V(t)$ as a Lyapunov function candidate can be written as

$$V\left(t\right) = \sum_{i=1}^{n}\left|e_i\left(t\right)\right|. \tag{46}$$

According to Lemma 5, the following inequality is obtained:

$$\begin{aligned} {}_0^C D_t^{\alpha} V\left(t\right) &= {}_0^C D_t^{\alpha}\sum_{i=1}^{n}\left|e_i\left(t\right)\right| \\ &\le \sum_{i=1}^{n}\operatorname{sgn}\left(e_i\left(t\right)\right){}_0^C D_t^{\alpha} e_i\left(t\right). \end{aligned} \tag{47}$$

And from expression (45) to (47), one has

$$\begin{aligned} {}_0^C D_t^{\alpha} V\left(t\right) &\le \sum_{i=1}^{n}\operatorname{sgn}\left(e_i\left(t\right)\right)\left\{-c_i e_i\left(t\right)\right. \\ &\quad - \sum_{j=1}^{n}\sum_{k=1}^{m} N_{ik}M_{kj}e_j\left(t\right) + \sum_{j=1}^{n}\left[\omega_{ij}\left[y_j\left(t\right)\right]g_j\left(y_j\left(t\right)\right)\right. \\ &\quad \left.\left. - \omega_{ij}\left[\xi x_j\left(t\right)\right]g_j\left(\xi x_j\left(t\right)\right)\right]\right\} = -c_i\sum_{i=1}^{n}\left|e_i\left(t\right)\right| \end{aligned}$$

$$+\sum_{i=1}^{n}\operatorname{sgn}(e_i(t))\sum_{j=1}^{n}\sum_{k=1}^{m}N_{ik}M_{kj}e_j(t)+\sum_{i=1}^{n}\operatorname{sgn}(e_i(t))\cdot\sum_{j=1}^{n}\left[\omega_{ij}\left[y_j(t)\right]g_j\left(y_j(t)\right)-\omega_{ij}\left[\xi x_j(t)\right]\cdot g_j\left(\xi x_j(t)\right)\right]\}. \tag{48}$$

Based on Assumptions 8 and 9, expression (48) can be written as

$$\begin{aligned}&{}_0^C D_t^\alpha V(t)\\&\le -c_i\sum_{i=1}^{n}|e_i(t)|+\sum_{i=1}^{n}|e_i(t)|\sum_{j=1}^{n}\sum_{k=1}^{m}\left|N_{jk}M_{ki}\right|\\&\quad+\sum_{i=1}^{n}\sum_{j=1}^{n}\left|e_j(t)\right|b^{\heartsuit}{}_{ij}G_j\\&=\sum_{i=1}^{n}|e_i(t)|\left[-c_i+\sum_{j=1}^{n}\sum_{k=1}^{m}\left|N_{jk}M_{ki}\right|+b^{\heartsuit}{}_{ij}G_j\right];\end{aligned} \tag{49}$$

from Assumption 18, $|b_{ji}{}^{\heartsuit}|=\max\{|b_{ji}^{*}|,|b_{ji}^{\circ}|\}$; and let $\varphi_i=c_i-\sum_{j=1}^{n}\sum_{k=1}^{m}|N_{jk}M_{ki}|-b^{\heartsuit}{}_{ij}G_j>0$, $\varphi=\min\{\varphi_i\}>0$; one has

$${}_0^C D_t^\alpha V(t)\le-\varphi_i\sum_{i=1}^{n}|e_i(t)|\le-\varphi V(t); \tag{50}$$

based on Lemma 15, an equilibrium point $e^*=0$ is the Mittag-Leffler stable, which means that system (37) is globally Mittag-Leffler stable, i.e., $\lim_{t\longrightarrow\infty}\|e(t)\|=0$. This completes the proof. □

Remark 20. According to Theorem 19, when $e(t)=y(t)-\xi x(t)$, the following form can be obtained:

$$\left\|y(t)-\xi x(t)\right\|\longrightarrow 0\quad(t\longrightarrow+\infty); \tag{51}$$

this means that the master system (17) and the slave system (20) achieve globally projective synchronization on account of the controller (40).

If $\xi=-1$, the control input (40) is designed as

$$\begin{aligned}u(t)&=u_q(t)+u_p(t)\\&=-(-D+C+NM)e(t)+(C-D)x(t)\\&\quad-A^*f(x(t))-\widehat{B}^*g(-x(t))-H-I\\&\quad-\sigma\operatorname{sgn}(S(t)),\end{aligned} \tag{52}$$

where the sliding surface $S(t)$ is designed by (31). A special case of Theorems 17 and 19 is obtained as follows.

Corollary 21. *Under Assumptions 8–18, the master system (17) and the slave system (20) are the globally asymptotic antisynchronization based on the controller (52).*

If $\xi=1$, the control input (40) is redesigned as

$$\begin{aligned}u(t)&=u_q(t)+u_p(t)\\&=-(-D+C+NM)e(t)-(C-D)x(t)\\&\quad+A^*f(x(t))-\widehat{B}^*g(x(t))-H+I\\&\quad-\sigma\operatorname{sgn}(S(t)).\end{aligned} \tag{53}$$

Corollary 22. *Assume that Assumptions 8–18 hold, the master system (17) and slave system (20) are the global asymptotically complete synchronization on account of the controller (53).*

If $\xi=0$, the sliding surface (31) is rewritten as

$$S(t)=y(t)+{}_0I_t^\alpha\left\{-\left[B^*g\left(y(t)\right)-\widehat{B}^*g(0)\right]+(C+NM)y(t)\right\}, \tag{54}$$

and the control input (40) is redesigned as

$$\begin{aligned}u(t)&=u_q(t)+u_p(t)\\&=-(-D+C+NM)y(t)-\widehat{B}^*g(0)-H\\&\quad-\sigma\operatorname{sgn}(S(t)).\end{aligned} \tag{55}$$

Corollary 23. *Under Assumptions 8–18, the slave system (20) is the globally asymptotically stabilized to the origin based on the controller (54).*

If the activation function and the parameters of slave system (20) are the same as master system (17), i.e.,

$${}_{t_0}^C D_t^\alpha y(t)=-Cy(t)+\breve{A}^*f\left(y(t)\right)+I+u(t), \tag{56}$$

where $\breve{A}^*=(\theta_{ij}[y_j(t)])_{n\times n}$, the sliding mode surface (31) is denoted as

$$\begin{aligned}S(t)&=e(t)\\&\quad+{}_0I_t^\alpha\left\{-\left[\breve{A}^*f(e(t)+\xi x(t))-\widehat{A}^*f(\xi x(t))\right]\right.\\&\quad\left.+(C+NM)e(t)\right\},\end{aligned} \tag{57}$$

where $\widehat{A}^*=(\theta_{ij}[\xi x_j(t)])_{n\times n}$; the control input (40) is rewritten as

$$\begin{aligned}u(t)&=u_q(t)+u_p(t)\\&=-NMe(t)+\xi A^*f(x(t))-\widehat{A}^*f(\xi x(t))\\&\quad+(\xi-1)I-\sigma\operatorname{sgn}(S(t)).\end{aligned} \tag{58}$$

Similar to Theorems 17 and 19, the following inference can be given.

Corollary 24. *The master system (17) and the slave system (56) are the globally projective synchronization based on the controller (58) if the Assumptions 8–18 hold.*

Remark 25. Chen, Zeng et al. [25] discussed the synchronization of FMNN based on the linear feedback controller. Bao & Cao [33] discussed the projective synchronization of identical fractional-order memristive neural networks by using adaptive feedback controller. But their results were about the same system. In fact, the parameters and functions of systems are variant due to environmental changes. Thus, our systems are general. In addition, the above control scheme cannot obtain projective synchronization of NFMNN. However, the fractional-order sliding mode controller can solve such problems in this paper. In a word, our system is general and our results achieve a valuable improvement.

4. Numerical Simulations

In this section, the results obtained in this paper are proved to be effectiveness and correctness by a numerical example.

Example 1. Consider the following three-dimensional FMNN as the master system and slave system:

$$\begin{aligned} {}_0^C D_t^\alpha x(t) &= -Cx(t) + Af(x(t)) + I \\ {}_0^C D_t^\alpha y(t) &= -Dy(t) + Bg(y(t)) + H + u(t), \end{aligned} \tag{59}$$

where $\alpha = 0.98$; $I = H = [0,0,0]^T$; the activation function $f(x(t)) = \tanh(|x(t)| - 1)$ and $g(y(t)) = \sin(|y(t)| - 1)$; $A = (a_{ij})_{n\times n}$ and $B = (b_{ij})_{n\times n}$; $i, j = 1, 2, 3$;

$$\mathrm{C} = \begin{bmatrix} 1.5 & 0 & 0 \\ 0 & 1.5 & 0 \\ 0 & 0 & 1.5 \end{bmatrix},$$

$$\mathrm{D} = \begin{bmatrix} 0.07 & 0 & 0 \\ 0 & 0.08 & 0 \\ 0 & 0 & 0.05 \end{bmatrix},$$

$$a_{11} = \begin{cases} -5 & |x_1| < 1 \\ -3 & |x_1| \geq 1, \end{cases}$$

$$a_{12} = \begin{cases} 5 & |x_2| < 1 \\ 6 & |x_2| \geq 1, \end{cases}$$

$$a_{13} = \begin{cases} 5 & |x_3| < 1 \\ 4.5 & |x_3| \geq 1, \end{cases}$$

$$a_{21} = \begin{cases} -9 & |x_1| < 1 \\ -7 & |x_1| \geq 1, \end{cases}$$

$$a_{22} = \begin{cases} 2 & |x_2| < 1 \\ 3 & |x_2| \geq 1, \end{cases}$$

$$a_{23} = \begin{cases} -1 & |x_3| < 1 \\ 3 & |x_1| \geq 1, \end{cases}$$

$$a_{31} = \begin{cases} -1 & |x_1| < 1 \\ 1 & |x_1| \geq 1, \end{cases}$$

$$a_{32} = \begin{cases} -9 & |x_2| < 1 \\ -8 & |x_2| \geq 1, \end{cases}$$

$$a_{33} = \begin{cases} 2 & |x_3| < 1 \\ 3 & |x_1| \geq 1, \end{cases}$$

$$b_{11} = \begin{cases} 0.45 & |y_1| < 1 \\ 0.33 & |y_1| \geq 1, \end{cases}$$

$$b_{12} = \begin{cases} -0.22 & |y_2| < 1 \\ -0.29 & |y_2| \geq 1, \end{cases}$$

$$b_{13} = \begin{cases} -0.2 & |y_3| < 1 \\ -0.25 & |y_3| \geq 1, \end{cases}$$

$$b_{21} = \begin{cases} -0.5 & |y_1| < 1 \\ -0.6 & |y_1| \geq 1, \end{cases}$$

$$b_{22} = \begin{cases} 0.19 & |y_2| < 1 \\ 0.25 & |y_2| \geq 1, \end{cases}$$

$$b_{23} = \begin{cases} -0.15 & |y_3| < 1 \\ 0.28 & |y_3| \geq 1, \end{cases}$$

$$b_{31} = \begin{cases} -0.11 & |y_1| < 1 \\ 0.11 & |y_1| \geq 1, \end{cases}$$

$$b_{32} = \begin{cases} 0.7 & |y_2| < 1 \\ 0.6 & |y_2| \geq 1, \end{cases}$$

$$b_{33} = \begin{cases} -0.21 & |y_1| < 1 \\ -0.275 & |y_1| \geq 1. \end{cases} \tag{60}$$

The measured output $z(t)$ is defined as $z(t) = Mx(t)$, where the parameter $M = [1,1,1]$. Next, the simulation diagram is given as follows.

Figure 1 describes phase diagram of master system (12) under the condition of initial value $x(0) = (1.1, 1.2, -1.5)^T$. Under the condition of initial value $y(0) = (-0.5, 1.5, -2.5)^T$, the phase trajectories of slave system (13) is showed in Figure 2 without the controller (41).

When the projective coefficient $\xi = -1$ and the gain matrix $N = (0.5, 0.3, 0.1)^T$, Figures 3 and 4 imply that the master-slave system (59) is globally asymptotic antisynchronization from Corollary 21 under the control scheme (52).

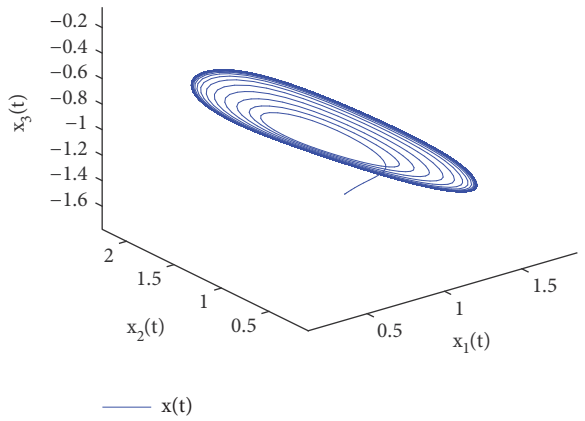

Figure 1: Phase plot of master system with initial condition $x(0) = (1.1, 1.3, -1.5)^T$.

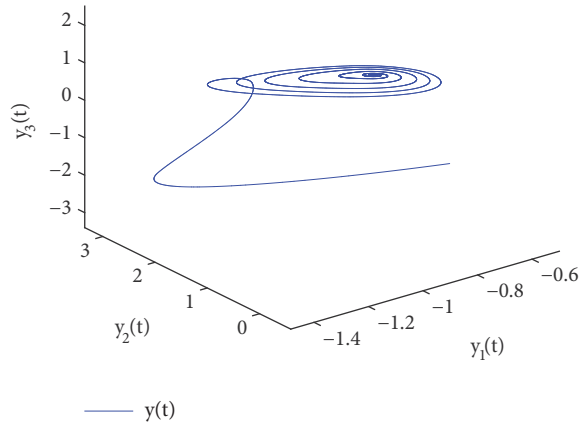

Figure 2: Phase plot of slave system with initial condition $y(0) = (-0.5, 1.5, -2.5)^T$ without the controller u(t).

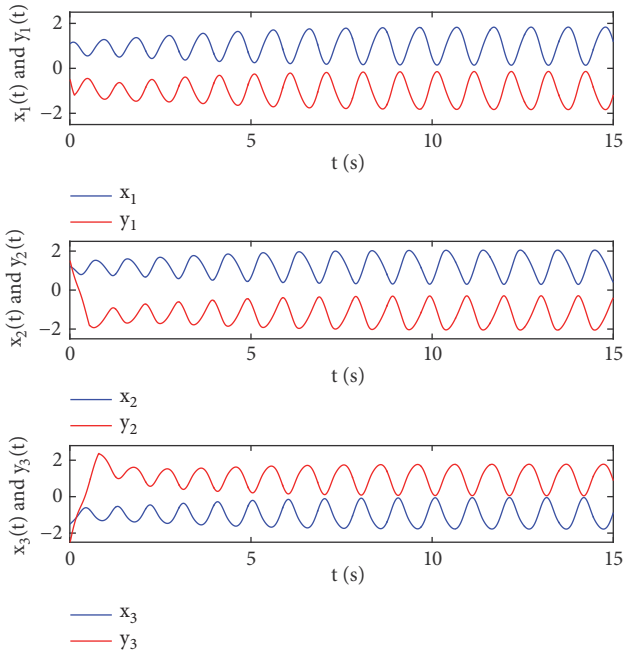

Figure 3: State trajectories of master-slave systems with ξ = -1.

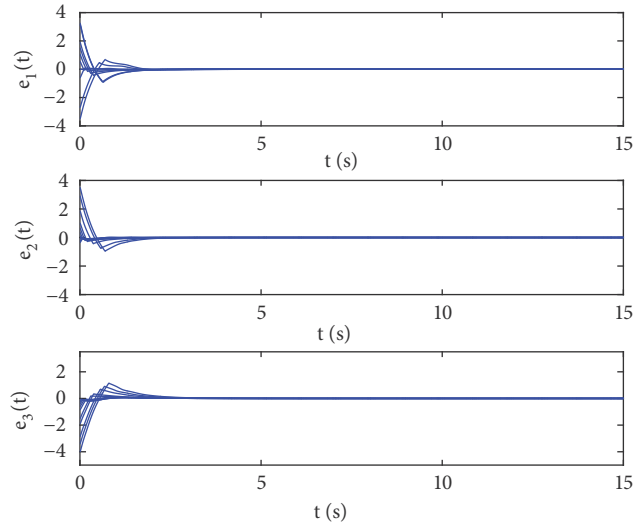

Figure 4: Select 10 random initial conditions and state trajectories of the synchronization errors $e_1(t)$, $e_2(t)$, and $e_3(t)$ with ξ =-1.

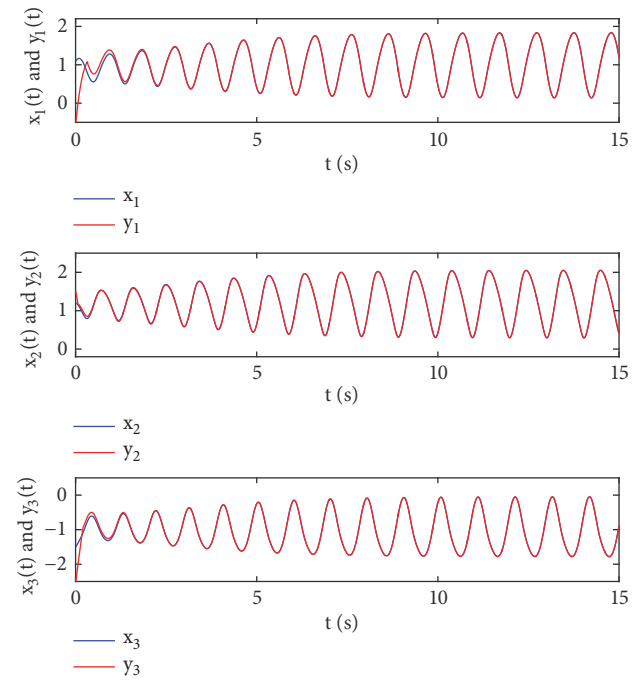

Figure 5: State trajectories of master-slave systems with $\xi = 1$.

Similarly, based on the control scheme (52) Figures 5 and 6 depict the simulation results for $\xi = 1$ with the gain matrix $N = (0.3, 0, 0)^T$, which indicate the master-slave (59) is globally asymptotically complete synchronization form Corollary 22.

In the following, the slave system of the globally asymptotically stabilized to the origin is considered based on the control scheme (54). In this case, $\xi = 0$ and $N = (-0.1, 0.3, -0.2)^T$. The Corollary 23 is illustrated in Figure 7.

Similarly, when $\xi = -2$ and the gain matrix $N = (0.4, -0.1, 0.1)^T$, the master-slave system (59) is globally

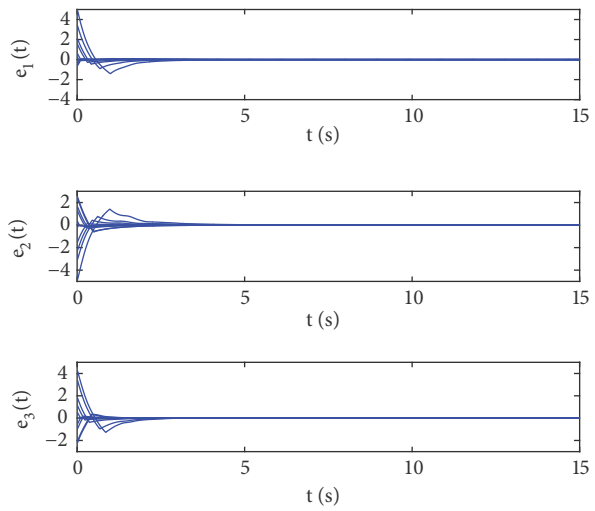

Figure 6: Select 10 random initial conditions and state trajectories of the synchronization errors $e_1(t)$, $e_2(t)$, and $e_3(t)$ with $\xi = 1$.

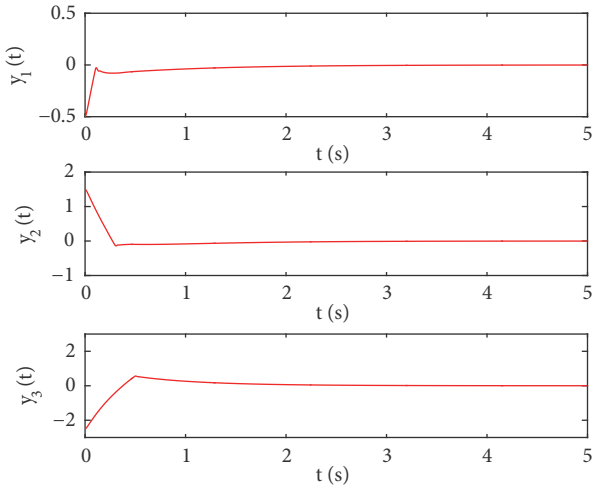

Figure 7: State trajectories of slave systems with $\xi = 0$.

asymptotically projective synchronization on the control scheme (40) which are showed in Figures 8 and 9.

When $\xi = 3$ and the gain matrix $N = (-0.1, -0.1, -0.1)^T$, Figures 10 and 11 show that the master-slave system is globally asymptotically projective synchronization under the control scheme (40).

5. Conclusion

In this paper, the problem of projective synchronization of NFMNN is studied. By designing a new type of fractional-order sliding mode controller and analyzing the reachability of sliding mode surface and the stability of sliding motion, the effective criteria for projective synchronization of NFMNN are obtained. Furthermore, the complete synchronization and antisynchronization of NFMNN, the stability of FMNN,

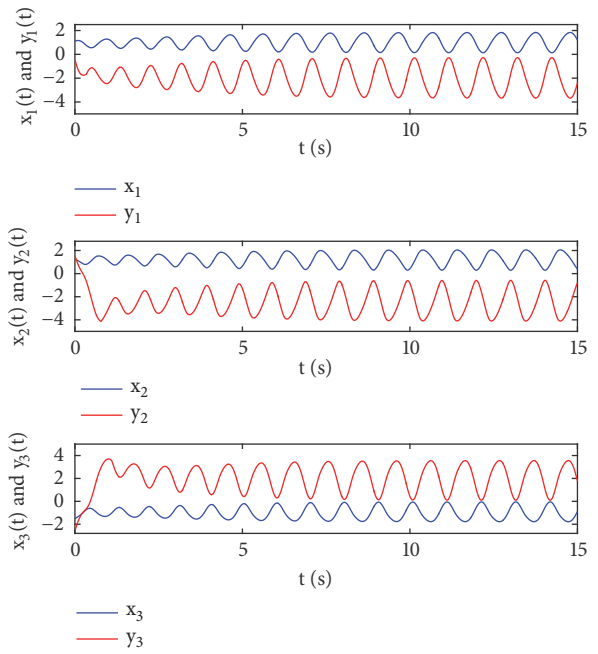

Figure 8: State trajectories of master-slave systems with $\xi = -2$.

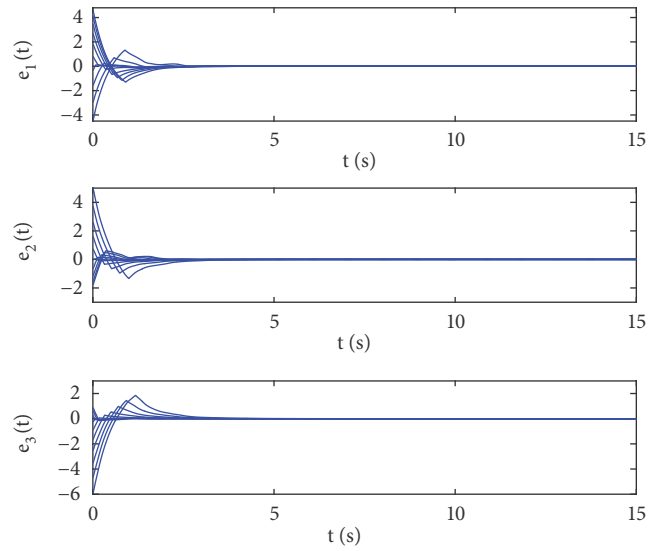

Figure 9: Select 10 random initial conditions and state trajectories of the synchronization errors $e_1(t)$, $e_2(t)$, and $e_3(t)$ with $\xi = -2$.

and the projective synchronization of the identical FMNN are special cases in this paper. In the future, we will consider the lag projective synchronization of NFMNN with delays.

Data Availability

The data used to support the findings of this study are available from the corresponding author upon request.

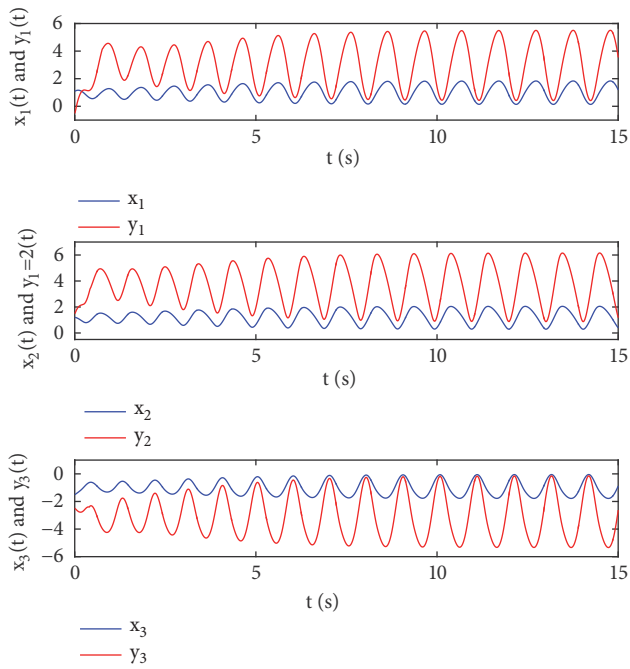

Figure 10: State trajectories of master-slave systems with $\xi = 3$.

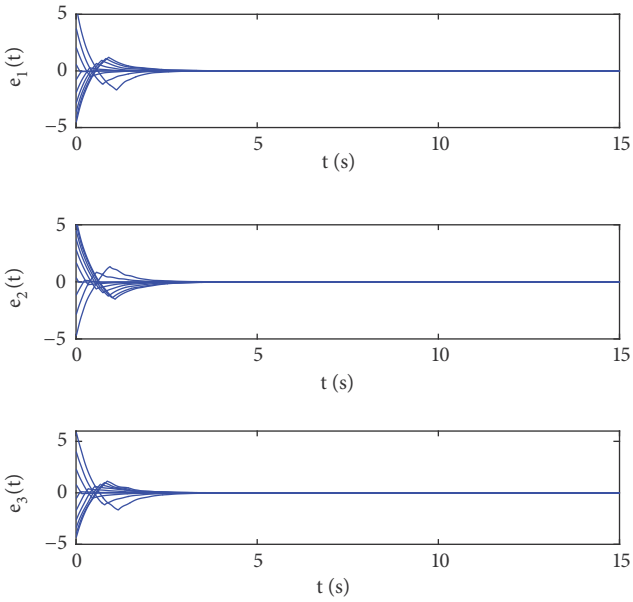

Figure 11: Select 10 random initial conditions and state trajectories of the synchronization errors $e_1(t)$, $e_2(t)$, and $e_3(t)$ with $\xi = 3$.

Conflicts of Interest

The authors declare that there are no conflicts of interest regarding the publication of this paper.

Authors' Contributions

Chong Chen carried out the main results and completed the corresponding proof. Zhixia Ding provides suggestions for the revision of the full text details. All authors read and approved the final manuscript.

Acknowledgments

This research is supported by National Science Foundation of China (61703312 and 61703313).

References

[1] L. O. Chua, "Memristor—the missing circuit element," *IEEE Transactions on Circuit Theory*, vol. 18, no. 5, pp. 507–519, 1971.

[2] L. O. Chua and S. M. Kang, "Memristive devices and systems," *Proceedings of the IEEE*, vol. 64, no. 2, pp. 209–223, 1976.

[3] L. O. Chua and C. Tseng, "A memristive circuit model for p-n junction diodes," *International Journal of Circuit Theory and Applications*, vol. 2, no. 4, pp. 367–389, 1974.

[4] D. B. Strukov, G. S. Snider, D. R. Stewart, and R. S. Williams, "The missing memristor found," *Nature*, vol. 453, pp. 80–83, 2008.

[5] S. H. Jo, T. Chang, I. Ebong, B. B. Bhadviya, P. Mazumder, and W. Lu, "Nanoscale memristor device as synapse in neuromorphic systems," *Nano Letters*, vol. 10, no. 4, pp. 1297–1301, 2010.

[6] F. Meng, B. Sana, Y. Li, Y. Liu, S. Lim, and X. Chen, "Bioengineered Tunable Memristor Based on Protein Nanocage," *Small*, vol. 10, no. 2, pp. 277–283, 2014.

[7] S. P. Adhikari, C. Yang, H. Kim, and L. O. Chua, "Memristor bridge synapse-based neural network and its learning," *IEEE Transactions on Neural Networks and Learning Systems*, vol. 23, no. 9, pp. 1426–1435, 2012.

[8] Y. N. Joglekar and S. J. Wolf, "The elusive memristor: properties of basic electrical circuits," *European Journal of Physics*, vol. 30, no. 4, pp. 661–675, 2009.

[9] J. Sun, Y. Shen, Q. Yin, and C. Xu, "Compound synchronization of four memristor chaotic oscillator systems and secure communication," *Chaos: An Interdisciplinary Journal of Nonlinear Science*, vol. 23, no. 1, Article ID 013140, pp. 1–11, 2013.

[10] B. Li, Y. Wang, Y. Chen, and H. Yang, "Training itself: Mixed-signal training acceleration for memristor-based neural network," in *Proceedings of the Asia and South Pacific Design Automation Conference (ASP-DAC)*, pp. 361–366, 2014.

[11] X. Hu, G. Feng, S. Duan, and L. Liu, "Multilayer RTD-memristor-based cellular neural networks for color image processing," *Neurocomputing*, vol. 162, pp. 150–162, 2015.

[12] S. Xiao, X. Xie, S. Wen, Z. Zeng, T. Huang, and J. Jiang, "GST-memristor-based online learning neural networks," *Neurocomputing*, vol. 272, pp. 677–682, 2018.

[13] C. Chen, L. Li, H. Peng, and Y. Yang, "Adaptive synchronization of memristor-based BAM neural networks with mixed delays," *Applied Mathematics and Computation*, vol. 322, pp. 100–110, 2018.

[14] J. D. Cao and R. X. Li, "Fixed-time synchronization of delayed memristor-based recurrent neural networks," *Science China Information Sciences*, vol. 60, no. 3, Article ID 032201, 2017.

[15] S. Wen, G. Bao, Z. Zeng, Y. Chen, and T. Huang, "Global exponential synchronization of memristor-based recurrent neural networks with time-varying delays," *Neural Networks*, vol. 48, pp. 195–203, 2013.

[16] Z. Ding, Z. Zeng, and L. Wang, "Robust finite-time stabilization of fractional-order neural networks with discontinuous

and continuous activation functions under uncertainty," *IEEE Transactions on Neural Networks and Learning Systems*, vol. 29, no. 5, pp. 1477–1490, 2018.

[17] Z. Ding, Z. Zeng, H. Zhang, L. Wang, and L. Wang, "New results on passivity of fractional-order uncertain neural networks," *Neurocomputing*, vol. 351, pp. 51–59, 2019.

[18] L. Chen, J. Cao, R. Wu, J. Tenreiro Machado, A. M. Lopes, and H. Yang, "Stability and synchronization of fractional-order memristive neural networks with multiple delays," *Neural Networks*, vol. 94, pp. 76–85, 2017.

[19] W. Liu, M. Jiang, and M. Yan, "Stability analysis of memristor-based time-delay fractional-order neural networks," *Neurocomputing*, vol. 323, pp. 117–127, 2019.

[20] A. Wu and Z. Zeng, "Global mittag-leffler stabilization of fractional-order memristive neural networks," *IEEE Transactions on Neural Networks and Learning Systems*, vol. 28, no. 1, pp. 206–217, 2017.

[21] G. Velmurugan, R. Rakkiyappan, and J. Cao, "Finite-time synchronization of fractional-order memristor-based neural networks with time delays," *Neural Networks*, vol. 73, pp. 36–46, 2016.

[22] H. Bao, J. Cao, and J. Kurths, "State estimation of fractional-order delayed memristive neural networks," *Nonlinear Dynamics*, vol. 94, no. 2, pp. 1215–1225, 2018.

[23] H. Bao, J. Cao, J. Kurths, A. Alsaedi, and B. Ahmad, "H∞ state estimation of stochastic memristor-based neural networks with time-varying delays," *Neural Networks*, vol. 99, pp. 79–91, 2018.

[24] L. M. Pecora and T. L. Carroll, "Synchronization in chaotic systems," *Physical Review Letters*, vol. 64, no. 8, pp. 821–824, 1990.

[25] J. Chen, Z. Zeng, and P. Jiang, "Global Mittag-Leffler stability and synchronization of memristor-based fractional-order neural networks," *Neural Networks*, vol. 51, pp. 1–8, 2014.

[26] A. Razminia and D. Baleanu, "Complete synchronization of commensurate fractional order chaotic systems using sliding mode control," *Mechatronics*, vol. 23, no. 7, pp. 873–879, 2013.

[27] J. Zhang, J. Wu, H. Bao, and J. Cao, "Synchronization analysis of fractional-order three-neuron BAM neural networks with multiple time delays," *Applied Mathematics and Computation*, vol. 339, pp. 441–450, 2018.

[28] M. Srivastava, S. P. Ansari, S. K. Agrawal, S. Das, and A. Y. Leung, "Anti-synchronization between identical and non-identical fractional-order chaotic systems using active control method," *Nonlinear Dynamics*, vol. 76, no. 2, pp. 905–914, 2014.

[29] L. P. Chen, Y. Chai, and R. C. Wu, "Lag projective synchronization in fractional-order chaotic (hyperchaotic) systems," *Physics Letters A*, vol. 375, no. 21, pp. 2099–2110, 2011.

[30] L. Zhang, Y. Yang, and F. wang, "Lag synchronization for fractional-order memristive neural networks via period intermittent control," *Nonlinear Dynamics*, vol. 89, no. 1, pp. 367–381, 2017.

[31] R. Martínez-Guerra and J. L. Mata-Machuca, "Fractional generalized synchronization in a class of nonlinear fractional order systems," *Nonlinear Dynamics*, vol. 77, no. 4, pp. 1237–1244, 2014.

[32] Z. Ding and Y. Shen, "Projective synchronization of nonidentical fractional-order neural networks based on sliding mode controller," *Neural Networks*, vol. 76, pp. 97–105, 2016.

[33] H.-B. Bao and J.-D. Cao, "Projective synchronization of fractional-order memristor-based neural networks," *Neural Networks*, vol. 63, pp. 1–9, 2015.

[34] H. Wu, L. Wang, Y. Wang, P. Niu, and B. Fang, "Global mittag-leffler projective synchronization for fractional-order neural networks: an lmi-based approach," *Advances in Difference Equations*, vol. 132, pp. 1–18, 2016.

[35] M. Zheng, L. Li, H. Peng, J. Xiao, Y. Yang, and H. Zhao, "Finite-time projective synchronization of memristor-based delay fractional-order neural networks," *Nonlinear Dynamics*, vol. 89, no. 4, pp. 2641–2655, 2017.

[36] V. K. Yadav, G. Prasad, M. Srivastava, and S. Das, "Combination–combination phase synchronization among non-identical fractional order complex chaotic systems via nonlinear control," *International Journal of Dynamics and Control*, vol. 7, no. 1, pp. 1–11, 2018.

[37] A. Chandrasekar and R. Rakkiyappan, "Impulsive controller design for exponential synchronization of delayed stochastic memristor-based recurrent neural networks," *Neurocomputing*, vol. 173, pp. 1348–1355, 2016.

[38] Y. Fan, X. Huang, Z. Wang, and Y. Li, "Improved quasi-synchronization criteria for delayed fractional-order memristor-based neural networks via linear feedback control," *Neurocomputing*, vol. 306, pp. 68–79, 2018.

[39] H. Bao, J. H. Park, and J. Cao, "Adaptive synchronization of fractional-order memristor-based neural networks with time delay," *Nonlinear Dynamics*, vol. 82, no. 3, pp. 1343–1354, 2015.

[40] Y.-H. Lan, H.-B. Gu, C.-X. Chen, Y. Zhou, and Y.-P. Luo, "An indirect Lyapunov approach to the observer-based robust control for fractional-order complex dynamic networks," *Neurocomputing*, vol. 136, pp. 235–242, 2014.

[41] I. Podlubny, *Fractional Differential Equations*, vol. 198 of *Mathematics in Science and Engineering*, Academic Press, New York, NY, USA, 1999.

[42] N. Aguila-Camacho, M. A. Duarte-Mermoud, and J. A. Gallegos, "Lyapunov functions for fractional order systems," *Communications in Nonlinear Science and Numerical Simulation*, vol. 19, no. 9, pp. 2951–2957, 2014.

[43] A. F. Filippov, "Differential equations with discontinuous right-hand side," in *Control Systems*, Kluwer, Dordrecht, The Netherlands, 1988.

[44] C. Edwards and S. Spurgeon, *Sliding Mode Control: Theory and Applications*, Taylor and Francis, London, UK, 1998.

[45] M. P. Aghababa, S. Khanmohammadi, and G. Alizadeh, "Finite-time synchronization of two different chaotic systems with unknown parameters via sliding mode technique," *Applied Mathematical Modelling*, vol. 35, no. 6, pp. 3080–3091, 2011.

[46] M. P. Aghababa, "A novel terminal sliding mode controller for a class of non-autonomous fractional-order systems," *Nonlinear Dynamics*, vol. 73, no. 1-2, pp. 679–688, 2013.